Autosomal Recessive Stickler Syndrome in Two Families Is Caused by Mutations in the *COL9A1* Gene

Konstantinos Nikopoulos,[1,2] *Isabelle Schrauwen,*[3] *Marleen Simon,*[4] *Rob W. J. Collin,*[1,2,5] *Marc Veckeneer,*[6] *Kathelijn Keymolen,*[7] *Guy Van Camp,*[3] *Frans P. M. Cremers,*[1,2] *and L. Ingeborgh van den Born*[6]

Purpose. To investigate *COL9A1* in two families suggestive of autosomal recessive Stickler syndrome and to delineate the associated phenotype.

Methods. The probands of two consanguineous autosomal recessive Stickler families were evaluated for homozygosity using SNP microarray in one and haplotype analysis in the other. Subsequently, the entire *COL9A1* open reading frame was analyzed by DNA sequencing in all members of the respective families. Several family members were investigated for dysmorphic features as well as ophthalmic, audiologic, and radiologic abnormalities.

Results. A novel homozygous *COL9A1* mutation (p.R507X) was identified in two affected Turkish sisters, and the previously published mutation (p.R295X) was found in a Moroccan boy. Ophthalmic assessment revealed myopia, cataracts, distinct vitreous changes, progressive chorioretinal degeneration, and exudative and rhegmatogenous retinal detachments. All three had sensorineural hearing loss and epiphyseal dysplasia. Intervertebral disc bulging was observed in one patient and in two heterozygous carriers of the p.R507X mutation.

Conclusions. A second, novel mutation was identified in *COL9A1*, causing autosomal recessive Stickler syndrome together with the previously described nucleotide change in two separate families. Although the overall phenotype was comparable to autosomal dominant Stickler, vitreous changes that may enable recognition of patients who are likely to carry mutations in *COL9A1* were identified, and exudative retinal detachment was observed as a new finding in Stickler syndrome. (*Invest Ophthalmol Vis Sci.* 2011;52:4774–4779) DOI:10.1167/iovs.10-7128

Stickler syndrome is a genetically heterogeneous connective tissue disorder that affects the ocular, skeletal, orofacial, and auditory systems. Mutations in three collagen genes, *COL2A1* (Stickler syndrome type I STL1 [MIM 108300]),[1] *COL11A1* (Stickler syndrome type II STL2 [MIM 604841]),[2] and *COL11A2* (Stickler syndrome type III STL3 [MIM 184840]),[3] have been shown to cause autosomal dominant Stickler syndrome. Yet, an autosomal recessive form of the disease, caused by a homozygous nonsense mutation in *COL9A1*, has been reported once in a consanguineous family of Moroccan origin.[4]

Clinical subclassification of Stickler syndrome is mainly based on vitreous changes, as the systemic features that can include premature osteoarthrosis, cleft palate, hearing impairment, and craniofacial abnormalities are highly variable, even within families and not specific to any gene locus. The most common form is STL1 caused by *COL2A1* mutations. Most of these patients display a congenital vitreous abnormality consisting of a vestigial gel in the retrolental space, bounded by a highly folded membrane (membranous or type I vitreous). STL2 patients with *COL11A1* mutations display a fibrillar and beaded appearance of the vitreous (fibrillar or type II vitreous). Recently, a third, more rare form was added, consisting of a hypoplastic vitreous that can be caused by mutations in *COL2A1* or *COL11A1*.[5] STL3 is a nonocular form of Stickler syndrome, because *COL11A2* is not expressed in the eye. Premature degenerative changes due to progressive liquefaction were noted in the autosomal recessive family with *COL9A1* mutations.[4] Since the incidence of rhegmatogenous detachments among Stickler patients is high, it is important to identify affected individuals through eye examination and direct genetic testing for confirmation of the diagnosis.

Here, we report on two families with an autosomal recessive form of the Stickler syndrome. Mutation analysis of the open reading frame (ORF) of *COL9A1* revealed one novel (c.1519C>T, p.R507X) and one previously reported (c.883C>T, p.R295X) nonsense nucleotide change. These two mutations were found in a homozygous state in the affected members of two families. Detailed clinical information on these families confirms the assumption by Van Camp et al.[4] that vitreous changes in patients with *COL9A1* mutations differ from those described in patients with *COL2A1* and *COL11A1* mutations.

From the Departments of [1]Human Genetics and [5]Ophthalmology, and the [2]Nijmegen Centre for Molecular Life Sciences, Radboud University Nijmegen Medical Centre, Nijmegen, The Netherlands; the [3]Department of Medical Genetics, University of Antwerp, Antwerp, Belgium; the [4]Department of Clinical Genetics, Erasmus Medical Centre, Rotterdam, The Netherlands; [6]The Rotterdam Eye Hospital, Rotterdam, The Netherlands; and the [7]Center for Medical Genetics, Universitair Ziekenhuis Brussel, Vrije Universiteit Brussel, Brussels, Belgium.

Supported by the Stichting Wetenschappelijk Onderzoek Oogziekenhuis Prof. Dr. H. J. Flieringa, Rotterdam; the European Union Research Training Network Grant RETNET MRTN-CT-2003-504003; the Algemene Nederlandse Vereniging ter Voorkoming van Blindheid, the F. P. Fischer Stichting; the Gelderse Blinden Stichting; the Landelijke Stichting voor Blinden en Slechtzienden; the Rotterdamse Vereniging Blindenbelangen, the Stichting Blindenhulp; the Stichting Blinden-Penning; the Stichting Nederlands Oogheelkundig Onderzoek, the Stichting OOG; the Stichting voor Ooglijders; the Stichting tot Verbetering van het Lot der Blinden, the Vereniging Bartiméus and the Fonds Wetenschappelijk Onderzoek (FWO), Vlaanderen.

Submitted for publication December 24, 2010; revised February 15, 2011; accepted February 16, 2011.

Disclosure: **K. Nikopoulos**, None; **I. Schrauwen**, None; **M. Simon**, None; **R.W.J. Collin**, None; **M. Veckeneer**, None; **K. Keymolen**, None; **G. Van Camp**, None; **F.P.M. Cremers**, None; **L.I. van den Born**, None

Corresponding author: L. Ingeborgh van den Born, The Rotterdam Eye Hospital, PO Box 70030, 3000 LM Rotterdam, The Netherlands; born@eyehospital.nl.

METHODS

Genetic Analysis

This study was approved by the ethics review boards of The Rotterdam Eye Hospital and the University of Antwerp and conformed to the Declaration of Helsinki. Informed consent was obtained from the participants before EDTA-anticoagulated venous blood was collected. Genomic DNA was isolated by using standard procedures.[6]

Homozygosity Mapping

Haplotyping was performed in one proband (family 2, II-1, Fig. 1) of the two consanguineous families using five highly polymorphic microsatellite markers (*D6S467*, *D6S254*, *D6S313*, *D6S1557*, and *D6S455*) covering a 2-cM region encompassing *COL9A1*. Capillary electrophoresis and pattern visualization of the fluorescently labeled PCR products were performed with an automatic DNA sequencer (model 3130XL; Applied Biosystems, Inc. [ABI], Foster City, CA). Allele sizes were then determined (GeneMapper V3.7 software; ABI).

The DNA of the proband (family 1, II-4; Fig. 1) of the other consanguineous family was genotyped using a SNP microarray platform (GeneChip Genome-Wide Human SNP Array 5.0; Affymetrix, Santa Clara, CA). Array experiments were conducted according to protocols provided by the manufacturer. Data from the SNP array analysis were genotyped with allied software (Genotype Console software; Affymetrix), whereas regions of homozygosity were calculated with another software program (Genomics Solution; Partek, St. Louis, MO).

Mutation Analysis

The ORF and the exon–intron junctions of the 38 exons of *COL9A1* were sequenced from forward and reverse strand initially in a proband from each of the two families (primer sequences available on request). Segregation studies of the identified mutations were performed in all available family members. Polymerase chain reaction (PCR) was executed according to the standard protocol. PCR products were purified (QiaQuick columns; Qiagen, Venlo, The Netherlands), either directly or after excision from the gel and were sequenced (model 3130XL sequencer with BigDye Terminator ver. 1.1 Cycle Sequencing Kit; ABI).

Clinical Diagnosis

We examined two consanguineous families with suspected autosomal recessive Stickler syndrome, one of Turkish and one of Moroccan descent. Both families were investigated for ophthalmic, audiologic, and radiologic abnormalities and dysmorphic features. All available retrospective data were studied.

In one of the two families that harbored *COL9A1* mutations (family 1), a more detailed ophthalmic assessment was performed, including best corrected visual acuity, biomicroscopy, ophthalmoscopy, and fundus photography. Fourier-domain optical coherence tomography (OCT) (RTVue; Optovue, Inc., Fremont, CA), was performed in two affected and two nonaffected members of family 1. In addition, scanning biometry (IOLMaster; Carl Zeiss Meditec, Jena, Germany), Goldmann perimetry, electrophysiology (ISCEV standards),[7] ultrasonography, and spectral-domain OCT (Spectralis; Heidelberg Engineering, Heidelberg, Germany) were obtained in the affected patients of family 1.

Audiologic examination included pure-tone audiometry performed with air conduction at 125, 250, 500, 1000, 2000, 4000, and 8000 Hz and bone conduction at 250, 500, 1000, 2000, and 4000 Hz in the two affected individuals of family 1 and their parents and the proband of family 2.

Radiographic data of the hips were available for all three affected persons (family 1, II-1 and II-4; family 2, II-1), and of the hands and knees in two patients (family 1, II-4; family 2, II-1). MRIs of the cervical spine and the cerebrum were available for one patient (family 1, II-4). MRI of the spine was obtained in the two heterozygous sisters of family 1 (II-2, II-3).

A general examination was performed by a clinical geneticist, and facial features were documented by photographs. Individual I-1 from family 1 died of a myocardial infarction during the project.

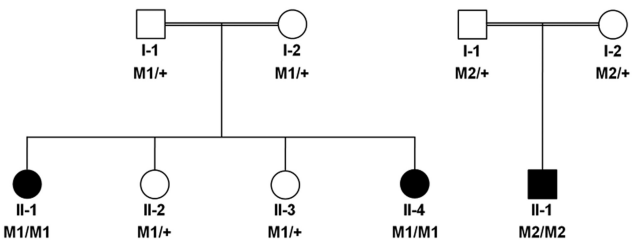

FIGURE 1. Complete pedigrees of families 1 and 2 with autosomal recessive Stickler syndrome and the segregation of the mutations identified in these families. *Filled symbols*: affected individuals; *open symbols*: nonaffected individuals. M1/M1, homozygous carriers of the p.R507X mutation; M1/+, heterozygous carriers of the p.R507X mutation; M2/M2, homozygous carriers of the p.R295X mutation; and M2/+, heterozygous carriers of the p.R295X mutation.

RESULTS

Genetic Analysis

Genome-wide SNP genotyping in patient II-4 of family 1 (Fig. 1), who is of Turkish descent, revealed three homozygous regions ≥10 Mb. A fourth homozygous region of 5.0 Mb, was located at chromosome 6, region q12-q11.1, between SNP_A-2144407 and SNP_A-1833968, encompassing *COL9A1.* In patient II-1 of family 2, who is of Moroccan descent, haplotype analysis also displayed a homozygous region spanning *COL9A1.* Sequence analysis revealed two homozygous *COL9A1* nonsense mutations: one novel (family 1: c.1519C>T, leading to p.R507X; Table 1, Fig. 1) and one known (family 2: c.883C>T, leading to p.R295X; Table 1; Fig. 1). The two heterozygous nucleotide changes were also identified in the nonaffected members of the two respective families.

Haplotype analysis of the Moroccan family (family 2) also showed that it not only shared the same mutation with the Moroccan family previously described, but also the identical disease haplotype in the 2-cM area encompassing *COL9A1* (data not shown), indicating a possible relationship.

Clinical Characteristics

Ophthalmic Findings. An overview of all the clinical data from families 1 and 2 is presented in Table 1. In family 1, individual II-1 was less severely affected than her younger sister (II-4). Both of them had moderate myopia before a photorefractive keratotomy was performed elsewhere. From the age of 21 onward, patient II-4 developed progressive epiretinal membranes with vitreoretinal traction, which led to an increasing number of telangiectatic vessels with small neovascularizations over the years and an exudative retinal detachment with Coats'-like vasculopathy in the right eye on recent examination (Fig. 2). The vitreous body in both affected sibs was partially liquefied and was distinctly divided by membranous veils, as seen on slit lamp examination and ultrasound. Epiretinal membranes with progressive vitreoretinal traction and retinoschisis were documented with OCT (Fig. 2). A progressive, chorioretinal degeneration was observed in both patients, leading to visual field defects and loss of rod–cone responses on electrophysiology. This was most pronounced in the younger sister with the exudative changes, whose ERG was almost nonrecordable (Fig. 3). Except for one abnormal, large vitreous floater in case II-2 of family 1, no ophthalmic abnormalities were observed in the heterozygotes on ophthalmoscopy and OCT.

Table 1. Clinical Features of All Members in Families 1 and 2 with Autosomal Recessive Stickler Syndrome

			Ophthalmology						
Patient	**Age**	***COL9A1* Genotype**	**VA: RE/LE***	**Refr:(D) RE/LE**	**Miscellaneous**	**Audiogram**	**Radiology**	**General features**	**Miscellaneous**
1/I-1	65 y	wt/R507X	N/T	N/T	N/T	SNHL 60 dB	N/T	Height: 1.65 m	Died of myocardial infarction
1/I-2	67 y	wt/R507X	0.7/0.5	Plano	Pseudophacic, normal vitreous, normal fundi.	SNHL 20 dB	N/T	Height: 1.58 m	Diabetes mellitus, hypertension
1/II-1	43 y	R507X/R507X	0.6/0.5	−6.25/−8.00 (24 y)†	Cataract extraction (32 y), axial length 25 mm‡, vitreous membranes; VR adhesions; paravascular retinal degeneration, retinoschisis; Goldmann: midperipheral sensitivity loss; ERG: reduced responses, OCT: VR traction, schisis.	Progressive SNHL	Coxa vara with short femoral necks and broad, flattened femoral heads; thoracolumbar scoliosis; degenerative vertebral changes; narrow disc space C5-6.	Height: 1.50 m, normal facial features, dysarthric speech, bilateral pes plano valgus, hypoplasia of the lateral femoral condyles, no hypermobile joints.	Spondylodesis due to thoracolumbar scoliosis (15 y), cholecystectomy (24 y).
1/II-2	41 y	wt/R507X	1.0/1.0	Plano	Clear lens, pronounced vitreous opacity (RE), normal fundi, OCT: normal.	N/T	Intervertebral disk bulging, Schmorl's nodules.	Height: 1.55 m, straightened lumbar lordosis, hypermobile joints.	None
1/II-3	36 y	wt/R507X	1.2/1.2	Plano	Clear lens, normal vitreous, normal fundi, OCT: normal.	N/T	Cervical hernia C5-6.	Height: 1.60 m, no hypermobile joints.	None
1/II-4	29 y	R507X/R507X	0.10/0.16	−6.50/−5.75 (18 y)†	Anterior chamber depth, 2.5 mm; axial length, 23.9 mm‡; subcapsular cataracts; vitreous membranes; VR traction; progressive retinal degeneration; Coats'-like exudative detachment (RE); Goldmann: constricted to 15°; ERG: ±nonrecordable, OCT: VR tractions, schisis.	Progressive SNHL	Coxa vara with short, broad femoral necks, normal knees/hands, cervical disc prolapse.	Height: 1.54 m, nasal/dysarthric speech, prominent supra orbital ridges, slightly sloping forehead, bilateral pes plano valgus, no hypermobile joints.	Subcortical frontal and temporal abnormalities CNS.
2/I-1	N/A	wt/R295X	N/T	N/T	N/T	N/T	N/T	Height: 1.74 m, no visual or hearing problems on history.	None
2/I-2	N/A	wt/R295X	N/T	N/T	N/T	N/T	N/T	Height: 1.63 m, no visual or hearing problems on history.	None
2/II-1	15 y	R295X/R295X	N/T	−18.5/−17	Bilateral amblyopia, bilateral RRD	Progressive SNHL	Short and squat metacarpals, short and broad femoral neck, irregular and flattened femoral epiphyses, small and squat iliac wing.	Short stature (3rd–10th percentiles), macrocephaly (60.6 cm), bilateral epicanthal folds, midfacial hypoplasia, class 3 malocclusion, no hypermobile joints.	None

Wt, wild type; y, years; D, diopters; RE, right eye; LE, Left eye; Goldmann, Goldmann kinetic perimetry; ERG, electroretinography; OCT, optical coherence tomography; VA, visual acuity; VR, vitreoretinal; N/T, not tested; Refr, refraction; RRD, rhegmatogenous retinal detachment. CNS, central nervous system; SNHL, sensorineural hearing loss.

* Visual acuity expressed in decimals.

† Refractive error before refractive surgery was performed.

‡ Axial length of the longest eye.

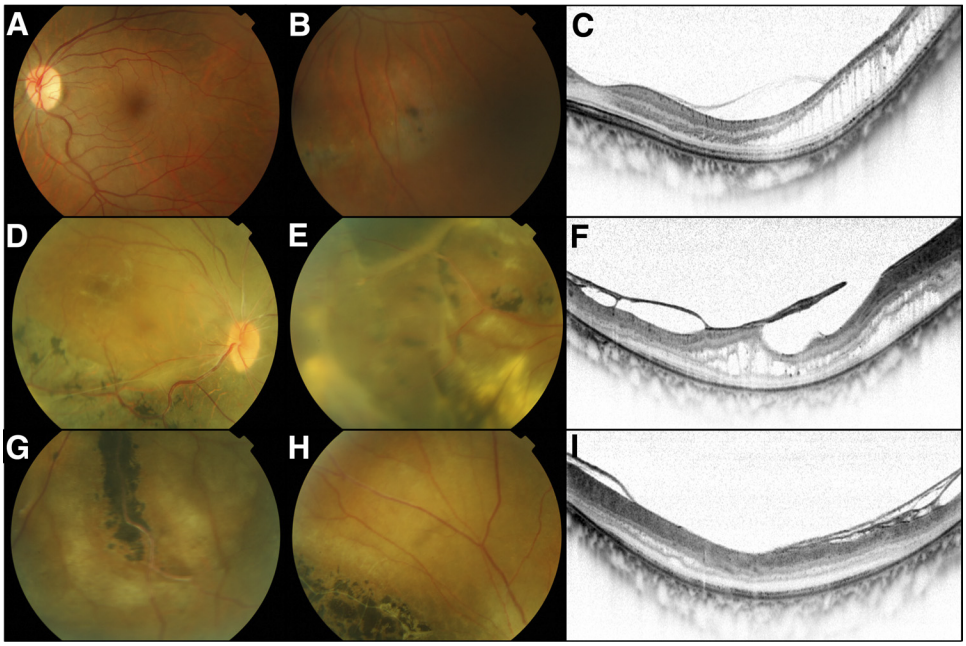

FIGURE 2. Fundus photographs and OCT in Stickler patients of family 1. (**A–C**) Patient II-1, 43 years old: fundus photographs of (**A**) the posterior pole of the left eye with no apparent abnormalities and (**B**) the periphery of the left eye, showed retinal degeneration. (**C**) OCT through the macular region of the left eye. Adhesion of the posterior hyaloid with vitreoretinal traction and schisis was apparent. (**D–I**) Patient II-4, 29 years old: fundus photographs of (**D**) the posterior pole of the right eye showed vascular sheathing, an epiretinal membrane, and chorioretinal degeneration along the vascular arcade and of (**E**) the periphery of the right eye revealing an exudative detachment with hard lipids. (**F**) OCT through the macular region of the right eye showed pronounced vitreoretinal traction and schisis. (**G**, **H**) Fundus photographs of the periphery of the left eye revealed paravascular lattice-like degeneration and epiretinal changes. (**I**) OCT superior to the macula of the left eye showed a thickened and split epiretinal membrane with retinal adhesions.

The index case of family 2 (II-1) showed bilateral amblyopia and myopia. He underwent several surgical procedures because of bilateral rhegmatogenous retinal detachments, making a description of the vitreous impossible.

Audiologic Findings. The hearing loss in the three patients from the two families with *COL9A1* mutations was moderate, sensorineural, and slightly progressive over the years, being most pronounced at higher frequencies, up to 110 dB in patient II-4 of family 1 (Fig. 4). The father (I-1) in family 1 also had a sensorineural hearing loss of the high tones of 60 dB at the age of 55 without a known cause. The mother (I-2) had a sensorineural hearing loss of 20 dB at the age of 58 years, which is within the normal range according to her age.

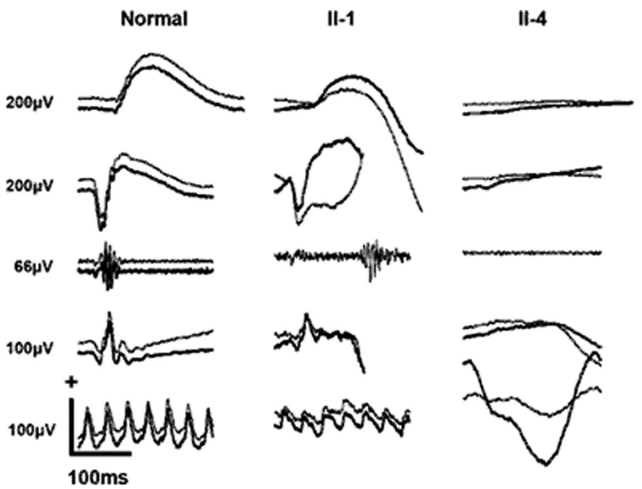

FIGURE 3. Standard ISCEV ERG recordings in a normal subject and in patients II-1 and II-4 of family 1. The recordings showed reduced scotopic and photopic responses in II-1 (LE>RE) and almost nonrecordable responses in II-4. In the 30-Hz flicker of II-4, an artifact is depicted that was caused by blinking.

General Features and Radiologic Findings. In the two affected members of family 1, several musculoskeletal alterations were detected, including slightly short stature, epiphyseal changes of the femoral head, a short femoral neck with coxa vara, and pes plano valgus without hypermobility of the joints (Fig. 5). X-rays of the spine showed a disc space narrowing at C5-6 and a thoracolumbar scoliosis with degenerative changes in patient II-1 and a herniation of the disc at C4-5 and C5-6 in patient II-4. Both of them had nasal, dysarthric speech. However, they did not have a cleft palate or micrognathia. Patient II-4 was slightly dysmorphic, with a round face and slightly low nasal bridge. At the age of 26, she had a sudden episode of headache with nausea, dizziness, and horizontal nystagmus. An MRI of the cerebrum showed aspecific subcortical abnormalities, frontal and temporal, without signs of cerebellar infarction.

Skeletal abnormalities were also noted in the two heterozygous sisters (II-2 and II-3) of family 1. Individual II-2 had back pain and a straightened lumbar lordosis. MRI of the lumbosacral spine showed diffuse intervertebral disc bulging at T12–L1, L1-2, and L4-5 and Schmorl's nodules. Patient II-3 had a cervical hernia at C5-6 on MRI.

Individual II-1 from family 2 was macrocephalic due to congenital hydrocephaly caused by an arachnoidal cyst with secondary stenosis of the aqueduct. He had a short stature, a

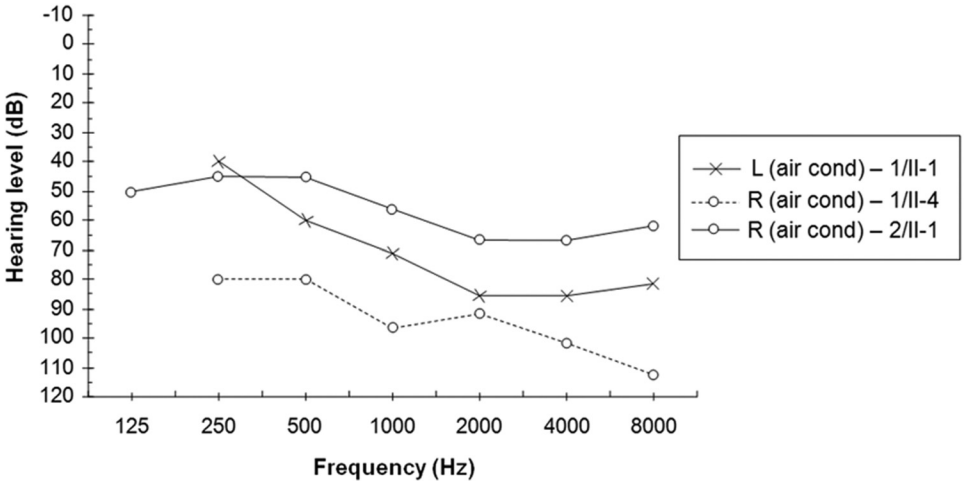

FIGURE 4. Audiogram with air conduction thresholds in the best ear of patients II-1 and II-4 from family 1 and patient II-1 from family 2. L, left ear; R, right ear; air cond, air conduction. 1/II-1 denotes patient II-1 from family 1, 1/II-4 denotes patient II-4 from family 1, and 2/II-1 denotes patient II-1 from family 2.

flat midface, and bilateral epicanthal folds. There was a class 3 malocclusion with mild deviation of the chin to the left. His neck was short with a low posterior hairline and he was not hypermobile. X-rays of the hips showed abnormalities of the femoral head and neck. His metacarpals were short and squat in contrast to patient II-4 (family 1) whose hands appeared normal on x-ray.

DISCUSSION

This study is the second report on the occurrence of autosomal recessive Stickler syndrome caused by *COL9A1* mutations. A novel, homozygous nonsense mutation (p.R507X) was detected in two Turkish sisters, and a previously reported homozygous nonsense mutation (p.R295X) was found in a Moroccan boy.

Stickler syndrome thus far seems to be caused solely by mutations affecting genes encoding the collagen types II, XI, and IX. In our families, we searched for characteristics that potentially could distinguish autosomal recessive Stickler patients with *COL9A1* mutations from patients with mutations in the genes (*COL2A1*, *COL11A1*, and *COL11A2*) causing the autosomal dominant form of the disease. The most important finding was the confirmation[4] that the vitreous structure does not match the Stickler type I and II phenotypes and the recently reported hypoplastic vitreous that are described in the dominant forms.[2,8–11] The vitreous in two of our patients contained membranous structures throughout its cavity, as seen in age-related degeneration. Furthermore, we documented vitreoretinal adhesions with progressive traction leading to chorioretinal degeneration, retinoschisis in the periphery and in the macular area and exudative and rhegmatogenous retinal detachment. Coats'-like exudative detachment in Stickler syndrome has not been reported in autosomal dominant cases. Rhegmatogenous detachments, on the other hand, may occur in up to 73% of STL1 patients who did not have prophylactic retinopexy[12] and in up to 42% of patients with STL2.[8]

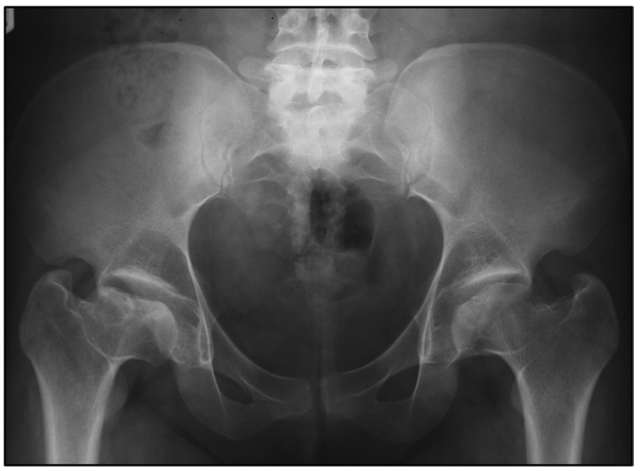

FIGURE 5. Radiograph of the hips of patient II-4 of family 1 at the age of 21. Note the coxa vara with short, broad femoral necks, the result of epiphyseal dysplasia.

Type IX collagen was the first member to be identified in a subgroup of collagens called FACITs (fibril-associated collagen with interrupted triples helices) and is encoded by *COL9A1*, *COL9A2*, and *COL9A3.* In the human vitreous, type IX collagen possesses a glycosaminoglycan (GAG) side chain covalently attached to its collagenous protein core[13] which renders it a proteoglycan. This side chain may play an important role stereochemically in the maintenance of the structure and spacing of adjacent collagen fibrils,[14,15] but also in the formation of the vitreous gel. Fibrillar collagens, such as type II or XI, tend to aggregate or fuse when they interact, and it has been shown that type IX collagen acts as a shield.[13] With aging, type IX collagen is progressively lost, minimizing the shielding effect and thus increasing the propensity of vitreous collagen fibrils to fuse, leading to synchysis as in our patients.

The nonocular symptoms in our families were very diverse, but all affected individuals had sensorineural hearing loss, epiphyseal dysplasia of the femoral heads with short femoral necks, and spinal abnormalities similar or even identical to the ones observed in autosomal dominant Stickler syndrome.[11,16] It is of note that the heterozygous mutation carriers (family 1: II-2 and II-3) were also symptomatic. None of the patients in our two families or in the one previously described[4] had a palatal cleft.

The overall clinical picture of our patients suggests that only the vitreous defects differ from those harboring mutations in *COL2A1* or *COL11A1*, and thus these may be used as a diagnostic criterion. Caution is necessary, though, since the vitreous phenotype is not always conclusive of involvement of a particular collagen,[5,17,18] and we could study the vitreous in only two siblings.

In the present families, homozygosity for a null mutation in *COL9A1* is associated with a full-blown Stickler phenotype, whereas the heterozygotes have milder skeletal phenotypes consistent with a mild effect of haploinsufficiency. Because of

a putative lower allele dosage, potentially producing a collateral, less severe clinical picture (e.g., skeletal problems), the latter could give an insight on the molecular etiology of the phenotype of the two heterozygous sisters. COL9A1 is involved in the formation of macromolecular complexes via a helical co-operative mechanism that does not progress unless the collagen concentration, at least in vitro, does not reach a critical threshold.[19] Haploinsufficiency in the *COL9A1* mutation carriers could explain a marginal or mediocre assembly of collagen molecules to form the heterotrimeric fibrils, possibly resulting in a partial phenotype. Mild clinical expression in heterozygous carriers of a recessive disease or of patients carrying two autosomal dominant mutations for a dominant trait being more severely affected has been described.[20]

Heterozygous splice site mutations leading to in-frame exon skipping in *COL9A1* and other *COL9* genes have been associated with multiple epiphyseal dysplasia (MED), a clinically highly heterogeneous disease.[21] The exon skipping (exon 8 and/or 10 in *COL9A1*, exon 3 *COL9A2/COL9A3*)[22–27] and subsequent deletion of several amino acids in the third collagenous domain, COL3, is compatible with a dominant-negative effect. Interestingly, the epiphyseal changes in COL9-associated MED result in more severe involvement of the knees, with relative sparing of the hips, whereas in our patients, the hips were involved, with sparing of the knees. In addition, *COL9A2* and *COL9A3* have been associated with intervertebral disc degeneration,[28] whereas the spinal changes in family 1 may also provide some indications for a role of *COL9A1* in intervertebral disc degeneration.

In summary, we identified a second novel mutation in *COL9A1* causing autosomal recessive Stickler syndrome, together with the previously described mutation in two separate families. Although their complete clinical picture was comparable to autosomal dominant Stickler, we were able to identify distinct phenotypic elements such as vitreous changes that might enable recognition of other patients who are likely to carry mutations in the *COL9A1* gene. Furthermore, we have added exudative retinal detachment to the spectrum of features characterizing the disease and indications that mutations in *COL9A1* may be associated with intervertebral disc degeneration.

Thus, patients with symptoms suggestive of autosomal recessive Stickler syndrome should be routinely checked for *COL9A1* changes, both for an accurate diagnosis and prognosis as well as for genetic counseling purposes.

Acknowledgments

The authors thank the patients for participating in this research, Han Brunner for valuable comments and discussion during the manuscript preparation, and Saskia D. van der Velde-Visser for expert technical assistance.

References

1. Williams CJ, Ganguly A, Considine E, et al. A −2→G transition at the 3′ acceptor splice site of IVS17 characterizes the COL2A1 gene mutation in the original Stickler syndrome kindred. *Am J Med Genet.* 1996;63:461–467.
2. Richards AJ, Yates JR, Williams R, et al. A family with Stickler syndrome type 2 has a mutation in the COL11A1 gene resulting in the substitution of glycine 97 by valine in alpha 1 (XI) collagen. *Hum Mol Genet.* 1996;5:1339–1343.
3. Vikkula M, Mariman EC, Lui VC, et al. Autosomal dominant and recessive osteochondrodysplasias associated with the COL11A2 locus. *Cell.* 1995;80:431–437.
4. Van Camp G, Snoeckx RL, Hilgert N, et al. A new autosomal recessive form of Stickler syndrome is caused by a mutation in the COL9A1 gene. *Am J Hum Genet.* 2006;79:449–457.
5. Richards AJ, McNinch A, Martin H, et al. Stickler syndrome and the vitreous phenotype: mutations in COL2A1 and COL11A1. *Hum Mutat.* 2010;31:E1461–E1471.
6. Miller SA, Dykes DD, Polesky HF. A simple salting out procedure for extracting DNA from human nucleated cells. *Nucleic Acids Res.* 1988;16:1215.
7. Marmor MF, Fulton AB, Holder GE, Miyake Y, Brigell M, Bach M. ISCEV Standard for full-field clinical electroretinography (2008 update). *Doc Ophthalmol.* 2009;118:69–77.
8. Poulson AV, Hooymans JMM, Richards AJ, et al. Clinical features of type 2 Stickler syndrome. *J Med Genet.* 2004;41:e107.
9. Richards AJ, Martin S, Yates JR, et al. COL2A1 exon 2 mutations: relevance to the Stickler and Wagner syndromes. *Br J Ophthalmol.* 2000;84:364–371.
10. Snead MP, Payne SJ, Barton DE, et al. Stickler syndrome: correlation between vitreoretinal phenotypes and linkage to *COL2A1*. *Eye (Lond).* 1994;8:609–614.
11. Snead MP, Yates JR. Clinical and molecular genetics of Stickler syndrome. *J Med Genet.* 1999;36:353–359.
12. Ang A, Poulson AV, Goodburn SF, Richards AJ, Scott JD, Snead MP. Retinal detachment and prophylaxis in type 1 Stickler syndrome. *Ophthalmology.* 2008;115:164–168.
13. Bishop PN, Holmes DF, Kadler KE, McLeod D, Bos KJ. Age-related changes on the surface of vitreous collagen fibrils. *Invest Ophthalmol Vis Sci.* 2004;45:1041–1046.
14. Scott JE. Proteoglycan: collagen interactions and subfibrillar structure in collagen fibrils: implications in the development and aging of connective tissues. *J Anat.* 1990;169:23–35.
15. Scott JE. The chemical morphology of the vitreous. *Eye.* 1992;6:553–555.
16. Rose PS, Ahn NU, Levy HP, et al. Thoracolumbar spinal abnormalities in Stickler syndrome. *Spine.* 2001;26:403–409.
17. McLeod D, Black GCM, Bishop PN. Vitreous phenotype: genotype correlation in Stickler syndrome. *Graefes Arch Clin Exp Ophthalmol.* 2002;240:63–65.
18. Parentin F, Sangalli A, Mottes M, Perissutti P. Stickler syndrome and vitreoretinal degeneration: correlation between locus mutation and vitreous phenotype: apropos of a case. *Graefes Arch Clin Exp Ophthalmol.* 2001;239:316–319.
19. Na GC, Butz LJ, Bailey DG, Carroll RJ. In vitro collagen fibril assembly in glycerol solution: evidence for a helical cooperative mechanism involving microfibrils. *Biochemistry.* 1986;25:958–966.
20. Zlotogora J. Dominance and homozygosity. *Am J Med Genet.* 1997;68:412–416.
21. Briggs MD, Chapman KL. Pseudoachondroplasia and multiple epiphyseal dysplasia: mutation review, molecular interactions, and genotype to phenotype correlations. *Hum Mutat.* 2002;19:465–478.
22. Bonnemann CG, Cox GF, Shapiro F, et al. A mutation in the alpha 3 chain of type IX collagen causes autosomal dominant multiple epiphyseal dysplasia with mild myopathy. *Proc Natl Acad Sci U S A.* 2000;97:1212–1217.
23. Holden P, Canty EG, Mortier GR, et al. Identification of novel pro-alpha 2 (IX) collagen gene mutations in two families with distinctive olgo-epiphyseal forms of multiple epiphyseal dysplasia. *Am J Hum Genet.* 1999;65:31–38.
24. Lohiniva J, Paassilta P, Seppanen U, Vierimaa O, Kivirikko S, Ala-Kokko L. Splicing mutations in the COL3 domain of collagen IX cause multiple epiphyseal dysplasia. *Am J Med Genet.* 2000;90:216–222.
25. Muragaki Y, Mariman EC, van Beersum SEC, et al. A mutation in COL9A2 causes multiple epiphyseal dysplasia (EDM2). *Ann N Y Acad Sci.* 1996;785:303–306.
26. Nakashima E, Kitoh H, Maeda K, et al. Novel COL9A3 mutation in a family with multiple epiphyseal dysplasia. *Am J Med Genet.* 2005;132A:181–184.
27. Paassilta P, Pihlajamaa T, Annunen S, et al. Complete sequence of the 23-kilobase human COL9A3 gene: detection of Gly-X-Y triplet deletions that represent neutral variants. *J Biol Chem.* 1999;274:22469–22475.
28. Kalichman L, Hunter DJ. The genetics of intervertebral disc degeneration. Associated genes. *Joint Bone Spine.* 2008;75:388–396.